Cell Reports, Volume *42*

Supplemental information

Single-cell transcriptomics illuminates regulatory steps driving anterior-posterior patterning of *Drosophila* embryonic mesoderm

Jingjing Sun, Chen Zhang, Fan Gao, and Angelike Stathopoulos

SUPPLEMENTAL INFORMATION

List of Supplemental Materials

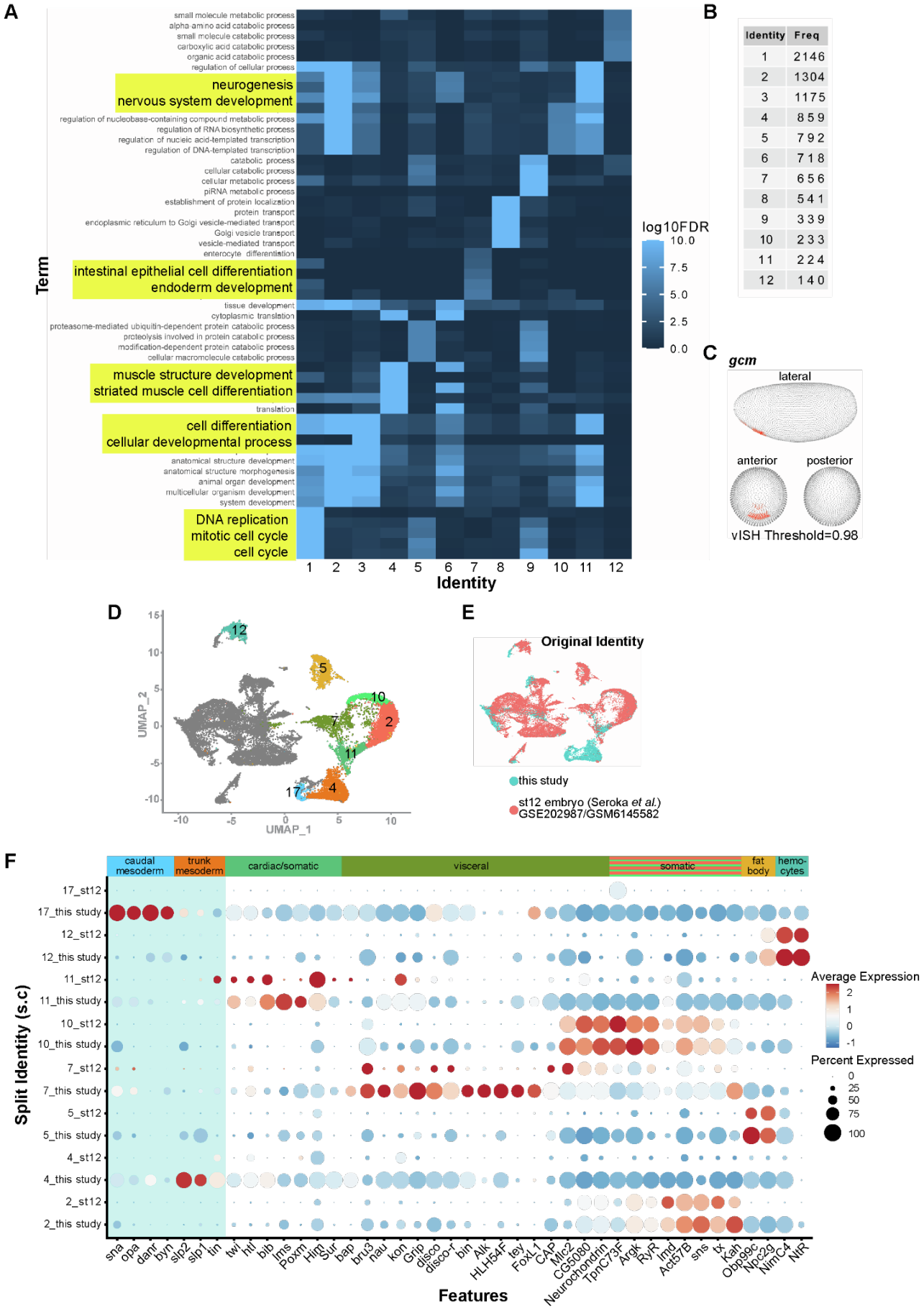
A
small molecule metabolic process
alpha-amino acid catabolic process
small molecule catabolic process
carboxylic acid catabolic process
organic acid catabolic process
regulation of cellular process
neurogenesis
nervous system development
regulation of nucleobase-containing compound metabolic process
regulation of RNA biosynthetic process
regulation of nucleic acid-templated transcription
regulation of DNA-templated transcription
catabolic process
cellular catabolic process
cellular metabolic process
piRNA metabolic process
establishment of protein localization
protein transport
endoplasmic reticulum to Golgi vesicle-mediated transport
Golgi vesicle transport
vesicle-mediated transport
enterocyte differentiation
intestinal epithelial cell differentiation
endoderm development
tissue development
cytoplasmic translation
proteasome-mediated ubiquitin-dependent protein catabolic process
proteolysis involved in protein catabolic process
modification-dependent protein catabolic process
cellular macromolecule catabolic process
muscle structure development
striated muscle cell differentiation
translation
cell differentiation
cellular developmental process
anatomical structure development
anatomical structure morphogenesis
animal organ development
multicellular organism development
system development
DNA replication
mitotic cell cycle
cell cycle
Term
1 2 3 4 5 6 7 8 9 10 11 12
Identity
log10FDR
10.0
7.5
5.0
2.5
0.0
B
Identity Freq
1 2146
2 1304
3 1175
4 859
5 792
6 718
7 656
8 541
9 339
10 233
11 224
12 140
C
gcm
lateral
anterior
posterior
vISH Threshold=0.98
D
UMAP_2
UMAP_1
12
5
10
2
7
11
17
4
E
Original Identity
this study
st12 embryo (Seroka et al.)
GSE202987/GSM6145582
F
caudal mesoderm
trunk mesoderm
cardiac/somatic
visceral
somatic
fat body
hemo-cytes
Split Identity (s.c)
17_st12
17_this study
12_st12
12_this study
11_st12
11_this study
10_st12
10_this study
7_st12
7_this study
5_st12
5_this study
4_st12
4_this study
2_st12
2_this study
sna opa danr byn slp2 slp1 tin twi htl bib Ims Poxm Him Sur bap bru3 nau kon Grip disco disco-r bin Alk HLH54F tey FoxL1 CAP Mlc2 CG5080 Neurochondrin TpnC73F Arpk RyR Imd Act57B sns tx Kah Obp99c Npc2g NimC4 NtR
Features
Average Expression
2
1
0
-1
Percent Expressed
0
25
50
75
100

Figure S1. Single-cell transcriptomes of gastrulating *Drosophila* embryos. Related to Figure 1, Tables S1 and S2.

(A) Gene ontology (GO) enrichment analysis of marker genes associated with each cluster.

(B) Number of cells in each cluster after removing the doublets and low-quality cells.

(C) Predicted expression pattern of *gcm* at stage 6 according to DVEX[S1] (https://shiny.mdc-berlin.de/DVEX/).

(D-F) Integration of the single cell transcriptomic data of gastrulation from this study with published data from stage 12 embryos[S2]. UMAP plot showing the mesodermal cell lineages s.c2, 4, 5, 7, 10, 11, 12, 17 (D) of the integrated datasets: (i) this study live wild-type (WT) #1 and (ii) st12 embryo from Seuroka *et al.* (see Methods). Contribution of integrated datasets to individual cell clusters: cells from this study in blue vs. cells from st12 published dataset in red (E). Side by side visualization of marker gene expression in mesoderm derived cell clusters from the integrated datasets by dotplot (F). Expression levels (normalized among the mesoderm cells) and percentage of cells in the cluster (y-axis) that express each selected marker (x-axis) are shown. Cells that express early caudal and trunk mesoderm genes are associated with s.c4 and s.c17 and predominantly identified by this study (F; see also D,E).

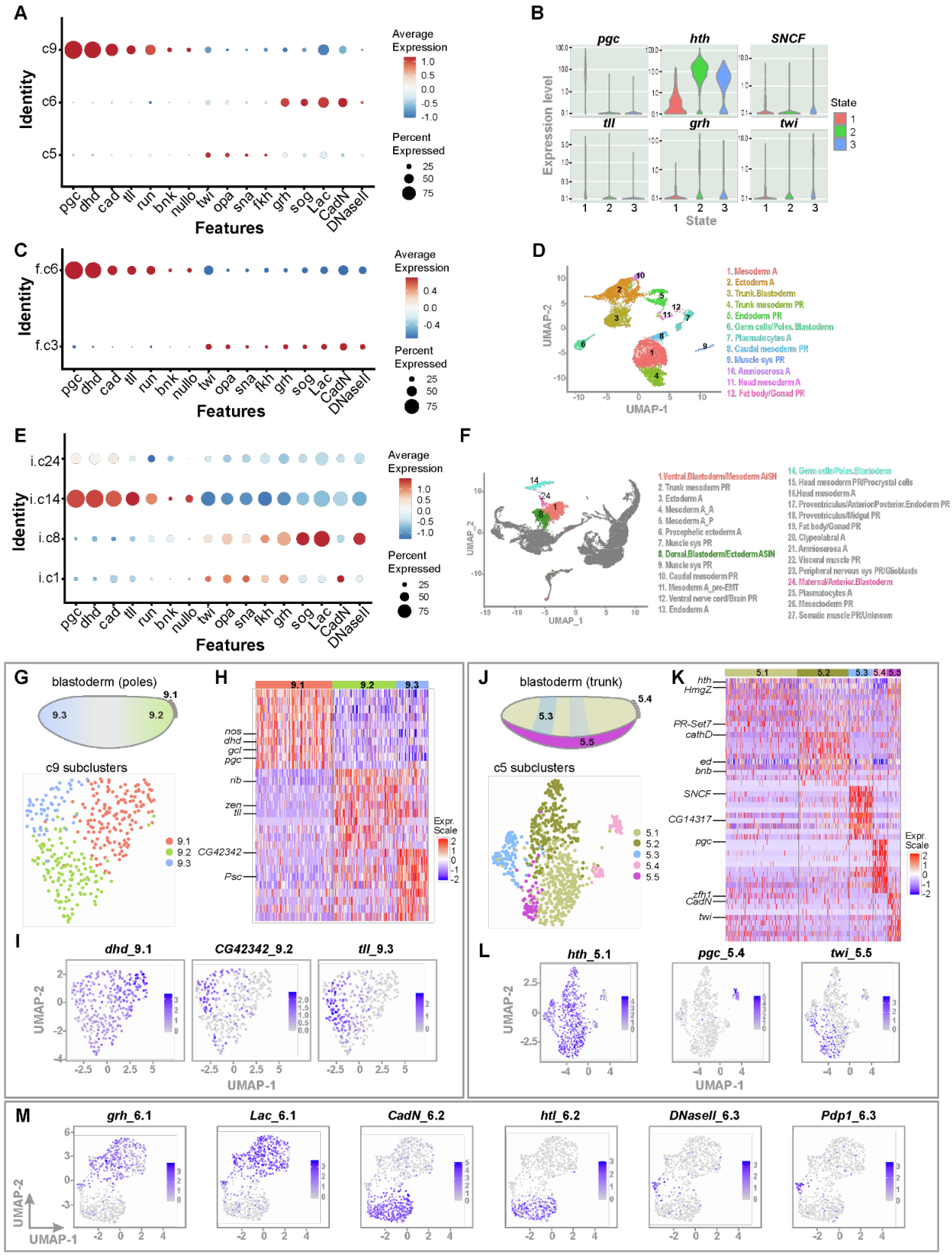

Figure S2. Featured gene expression during nc14. Related to Figure 2 and Tables S3-5.

(A) Dotplot showing representative gene expression in the cell clusters associated with three blastoderm-associated cell clusters of live WT#1 dataset (A).

(B) Violin plots showing expression of additional markers associated with the three cell states generated by trajectory analysis of c9, 5, 6 (Related to Figure 2E,F).

(C,D) Single cell transcriptomic profiling of methanol-fixed cells isolated from stage 5-10 embryos identified 12 cell clusters (D) that largely overlap with those from the live cells (A; live WT#1 shown in main text figures). (C) Dotplot showing expression of the same markers in the two blastoderm-associated cell clusters of fixed cell experiment (fixed WT#3 clusters: f.c3 and f.c6).

(E,F) Four blastoderm-associated cell clusters emerge (i.c1, i.c8, i.c14, i.c24) as a result of integrating three independent single-cell datasets: live WT#1, live WT#2, and fixed WT#3 (E; see Methods). Violin plot showing the trend of representative gene expression in the 27 cell clusters identified by PC analysis in which blastoderm cell clusters are highlighted (F).

(G-I) UMAP plot (G) and heatmap (H) of c9 cells from live WT#1 data (main text figures), which are divided into three subclusters (c9.1, c9.2 and c9.3). Diagram illustrates a blastoderm embryo with color-coded domains labeled with associated subclusters. (I) Subclustering UMAP plots of selected gene expression.

(J-L) UMAP plot (J) and heatmap (K) of c5 cells from live WT#1. Five subclusters (c5.1-5.5) are identified. Color-coded domains of the schematic blastoderm embryo are labeled with associated subcluster identity. (L) Subclustering UMAP plots of selected gene expression.

(M) Subclustering UMAP plots showing selected marker gene expression associated with the three subclusters identified in c6 from live WT#1 (see Figure 2K).

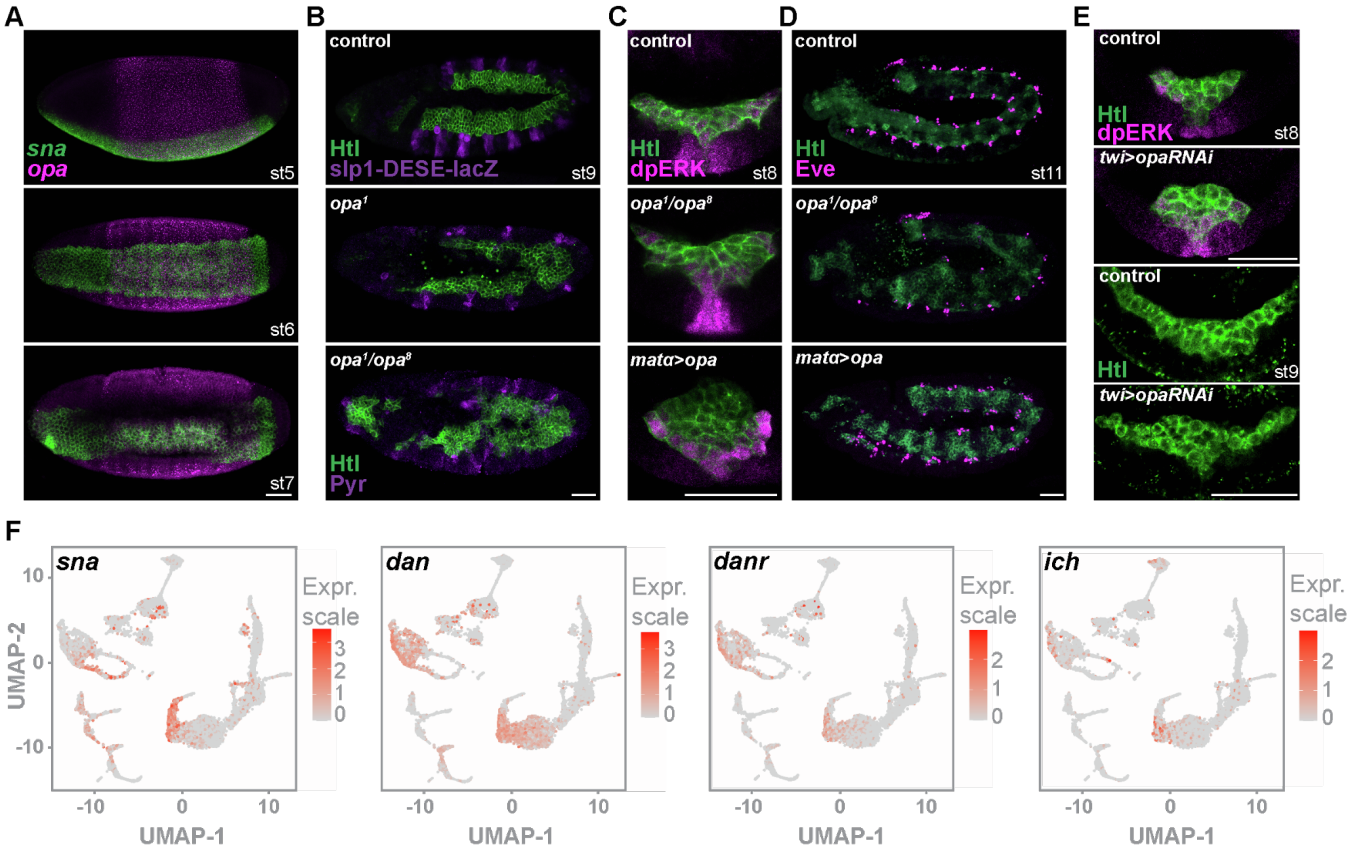

Figure S3. Pre-EMT expression of Opa contributes to mesoderm patterning and lineage differentiation and overexpression of *opa* in the mesoderm disrupts its normal development. Related to Figure 3.

(A) Detection of *opa* transcripts (purple) in the mesoderm (labeled by *sna* probe in green) during invagination.

(B-E) Mesoderm patterning associated with dysregulated *opa* expression. Whole mount side views and Cross sections showing spreading and differentiation defects in *opa* loss of function and overexpression mutants (B-D). Mesoderm cells are labeled with an anti-Htl antibody (green), dpERK antibody staining (purple, C) was used to assay active RTK signaling and Eve antibody (purple, D) to mark the pericardial cells. *opa* mutants exhibit uneven distribution of mesoderm cells and reduced numbers of *slp1* stripes as indicated by β-Galactosidase staining (dark purple, B). Spreading is asymmetric and a delay in spreading is observed in *matα>opa* embryos. The mesoderm spreading defect in these mutants leads to a reduction in the number of pericardial cells at stage 11. When *opa* is specifically knocked-down in the mesoderm by *twi(2xPE)GAl4* (see Methods), only minor mesoderm spreading defects were observed at st8-9 (E), and pericardial cell distribution appears normal.

(F) UMAP plots of *sna*, *dan*, *danr* and *ich* with red intensity indicating the relative expression levels.

Genotypes and developmental stages are as indicated. Scale bars=50μm.

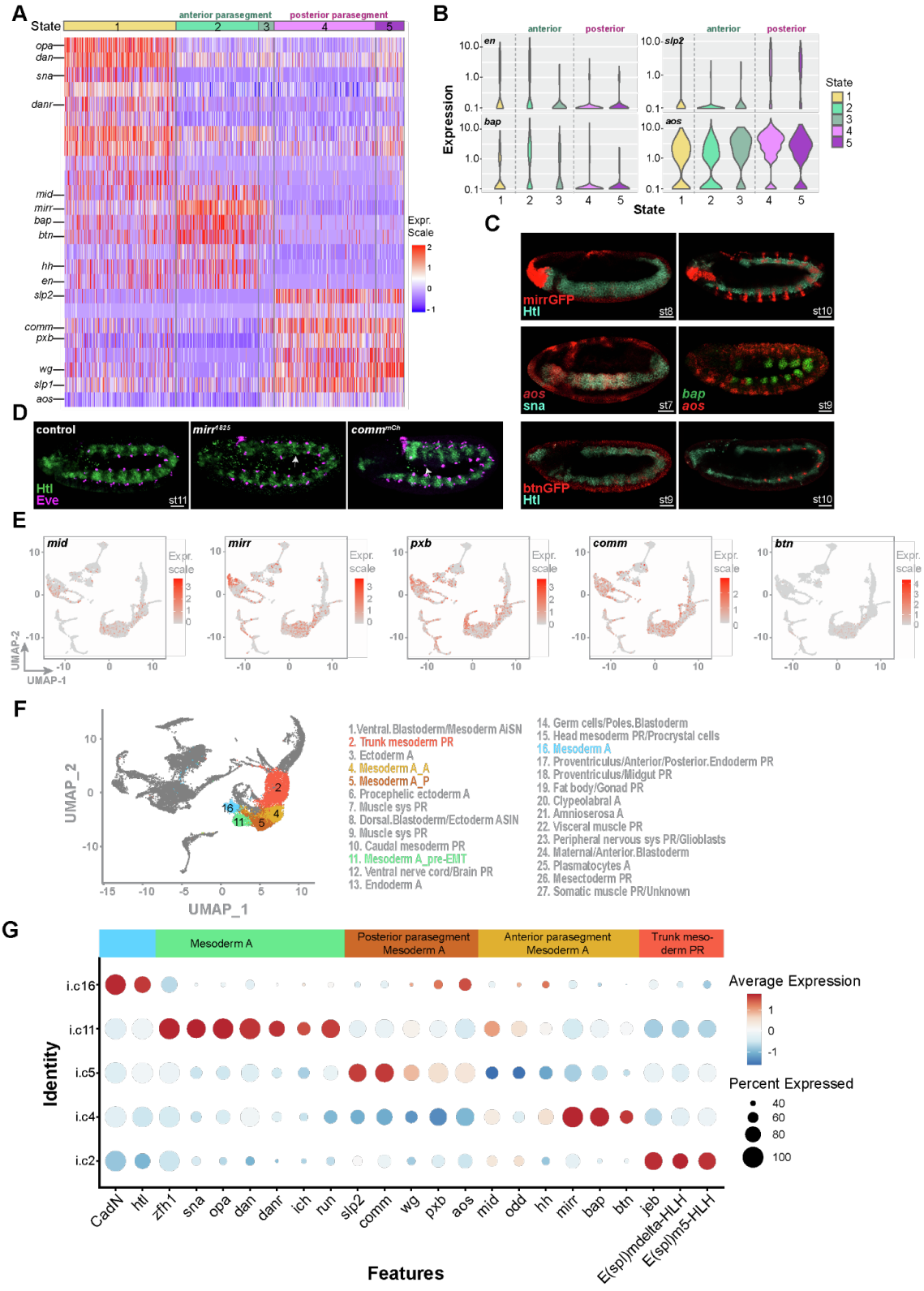

Figure S4. Trajectory analysis of c1 mesoderm cells illuminates patterning along the A-P axis. Related to Figure 4, Tables S5 and S6.

(A-B) Trajectory analysis generates a heatmap showing the top ten marker genes of each five cellular states (A). Violin plots of additional marker gene expression are shown in (B).

(C) Antibody staining of GFP-tagged *mirr* and *btn* or in situ hybridization for endogenous *aos* and *bap* to confirm their segmented expression patterns in st7-10 embryos.

(D) Expression of *mirr* and *comm* in the mesoderm is required for proper cardiac progenitor cells specification. Arrows indicate the missing and extra Eve-positive cell cluster in the *mirr* and *comm* mutant embryos.

(E) UMAP plots of selected markers with red intensity indicating relative expression levels.

(F,G) Five cell clusters (i.c2, 4, 5, 11, 16) relating to the trunk mesoderm are highlighted in the UMAP of integrated single cell datasets (F). Expression of mesoderm markers are shown in the dotplot (G). Three clusters from thes integrated dataset (i.e. i.c4, 5, 11) are equivalent to c1 of live WT #1 (the dataset focused on in this study).

Scale bars=50μm.

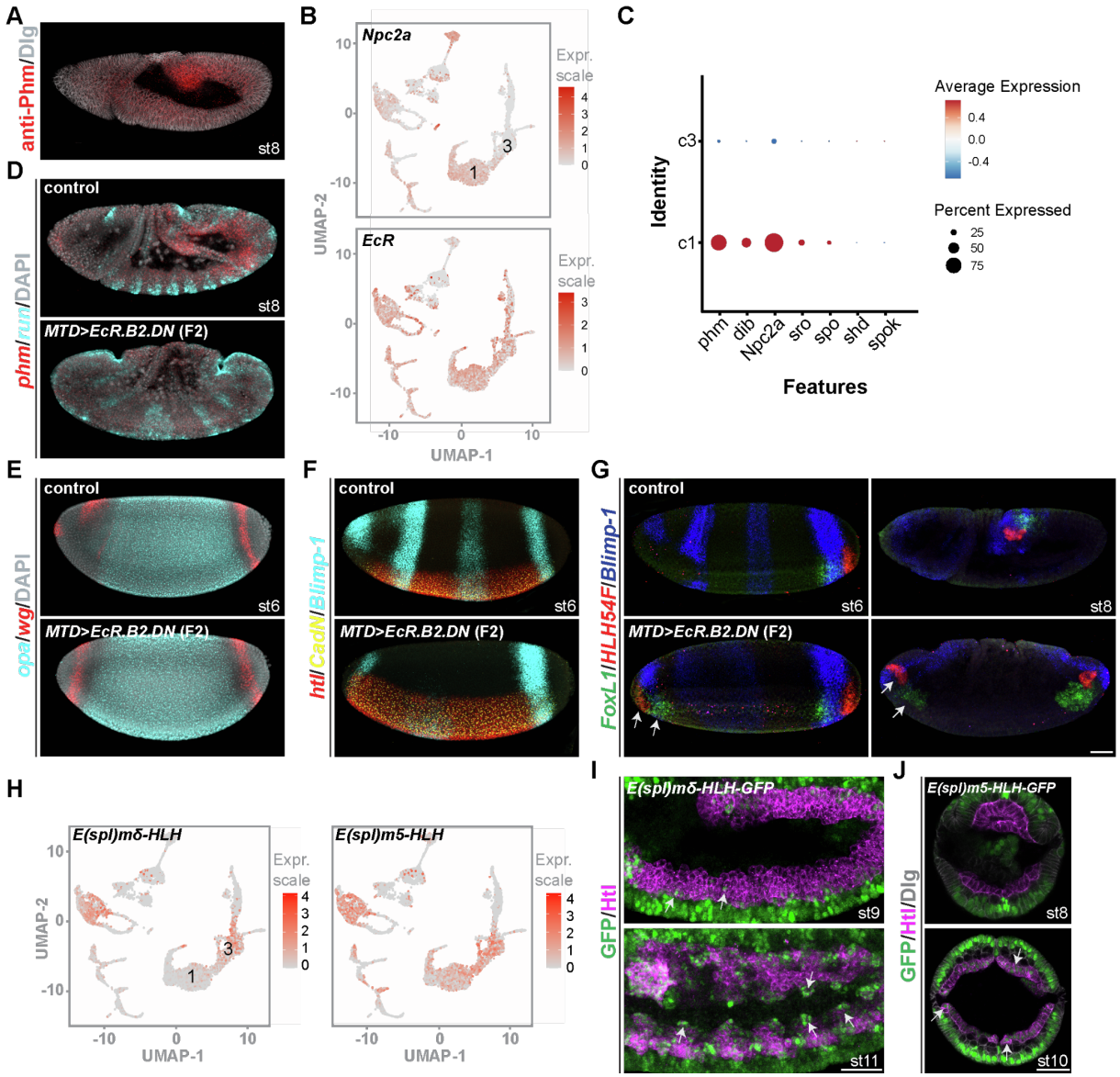

Figure S5. Patterning defects in maternal EcR dominant negative mutants and upregulation of Notch signaling targets post EMT. Related to Figure 5.

(A) Phm (red) and Dlg (white, labeling basolateral cell membranes) antibody staining of wild-type embryo showing Phm is expressed in the mesoderm at st8.

(B) Global UMAPs of *Npc2a* and *EcR*.

(C) Dotplot showing selected Halloween gene expression in mesoderm cell clusters c1 and c3.

(D-G) Defects in AP patterning are observed in F2 second generation offspring when a dominant negative form of EcR is maternally-expressed in the ovary using *MTD-GAL4*. *phm* is downregulated, and a posterized anterior domain is visible in the *MTD>EcR.DN* (F2) mutant (D). (E-G) Disrupting EcR function maternally leads to the anterior domain of embryos adopting gene expression patterns resembling the posterior domain (E), without affecting D-V patterning and mesoderm specification (F). Duplication of the posterior *wg* stripe (red) and slight anterior expansion of *opa* trunk expression (light blue) are seen in the mutant (E). Furthermore, in these mutants,

the anterior and central *Blimp-1* stripes are lost (cyan, F; see also dark blue, G). Duplicated expression of the posterior trunk mesoderm genes *FoxL1* (green) and *HLH54F* (red) is also associated with maternal expression of *EcR.DN* (arrows, G).

(H-J) *E(spl)* complex genes are upregulated in c3 post-EMT mesoderm (H), as confirmed by immunostaining of GFP-tagged *mδ-HLH* (arrows, I, side view of whole-mount embryos are shown) and *m5-HLH* (arrows, J cross-sections are shown).

Combinations of genes and developmental stages assayed by in situ hybridization are as indicated. Scale bars=50μm.

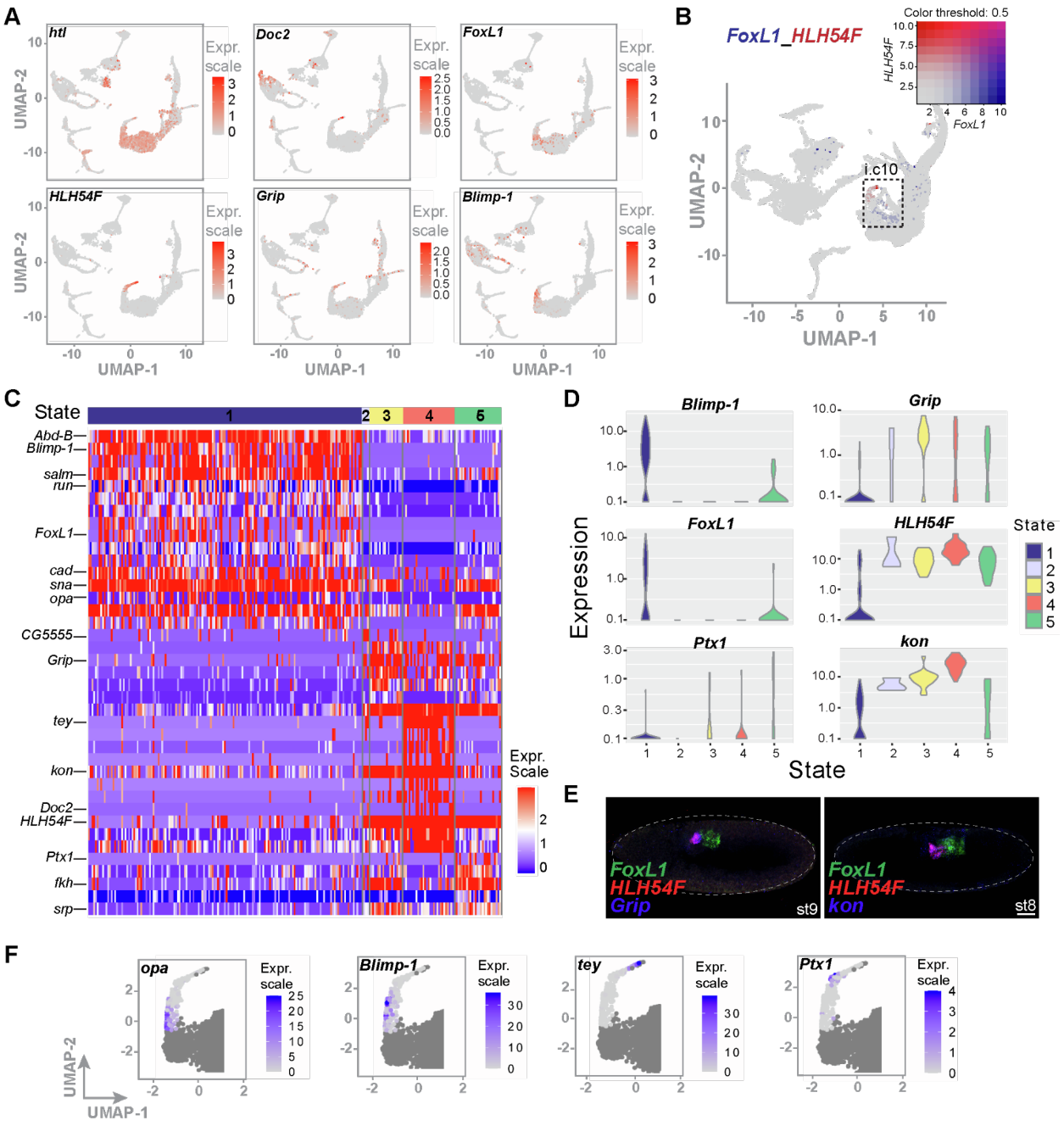

Figure S6. Transcription programs that specify the posterior trunk mesoderm. Related to Figure 6 and Table S7.

(A) UMPAs of selected marker genes in c10.

(B) UMAP plot showing expression of *FoxL1* (blue) and *HLH54F* (red) simultaneously in the integrated dataset (live WT#1, live WT#2 and fixed WT#3). Caudal mesoderm cluster i.c10 is marked by the dotted line box. Expression scale showing to the right.

(C-F) Trajectory analysis of c10 identifies five different cellular states. Heatmap of the top 10 marker genes for each state (C). Violin plots of selected markers with colors labeling different cellular states (D). Consistent with the trajectory analysis, *Grip* and *kon* (blue) are co-expressed with *HLH54F* (red) in the CVM precursors while distinct

from the *FoxL1*-expressing cells (green) at st8-9 (E). Cropped UMAP plots for selected cell state markers showing *opa* and *Blimp-1* (both state 1), *tey* (state 4) and *Ptx1* (state 5) occupy distinct space within c10 (F). Scale bar=50μm.

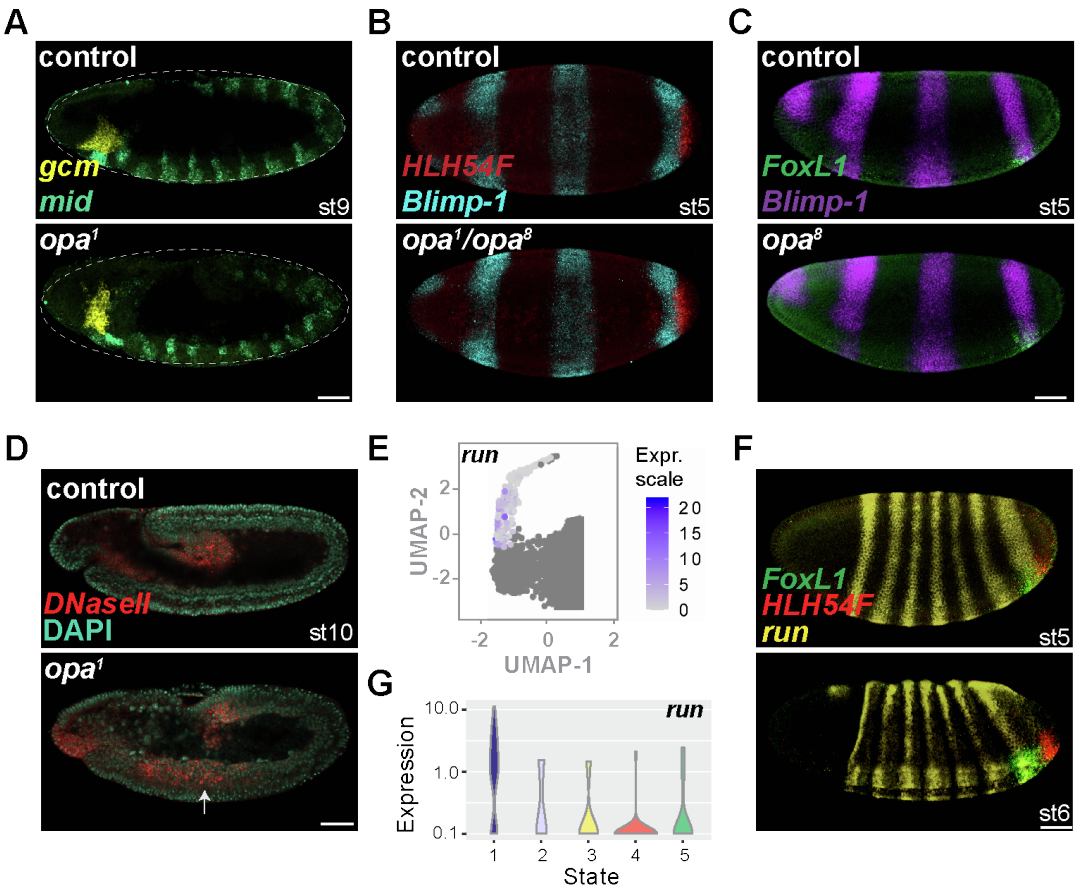

Figure S7. *opa* functions together with other factors in the trunk to spatially restrict gene expression to the head and caudal mesoderm. Related to Figure 7.

(A-C) Loss of *opa* does not lead to obvious changes in *gcm* (A, yellow), *HLH54F* (B, red) and *FoxL1* (C, green) expression.

(D) Ectopic expression of *DNaseII* (red) is observed in the trunk in the *opa*^{1} mutant (arrow, D) suggesting Opa (directly or indirectly) normally supports repression of this gene from the trunk.

(E-G) Pair rule gene *run* is enriched in state 1 cells from trajectory analysis (G) within c10 (E). Cells comprising c10 state 1 also are associated with *FoxL1* transcripts (see Figures 6B, S6D). This result and the overlapping expression of *run* and *FoxL1* at stage 5 detected by *in situ* hybridization using HCR probes (F) suggested a role for Run in supporting *FoxL1* expression.

Genes detected and stages are as labeled. Scale bars=50μm.

Table S8, List of oligonucleotides used in this study, related to key resources table

Oligonucleotides (Table S8)		
D2eGFP RNA probe (HCR)	Molecular Instruments	d21260aa-84e9-4ae2-9adf-109eef0e85eb/PRH935
HLH54F RNA probes (HCR)	Molecular Instruments	4358/E576
FoxL1 RNA probes (HCR)	Molecular Instruments	fd9e7d98-87b2-46e2-967a-a384167b8da6/PRR051
Blimp-1 RNA probes (HCR)	Molecular Instruments	fd9e7d98-87b2-46e2-967a-a384167b8da6/PRR053
Doc2 RNA probes (HCR)	Molecular Instruments	5c204473-08ca-4546-bf24-1925b8003083/PRO669
kon RNA probes (HCR)	Molecular Instruments	4049/E192
Grip RNA probes (HCR)	Molecular Instruments	9d28cc4d-0e82-4330-9564-96b40a58248c/RTB563
hkb RNA probes (HCR)	Molecular Instruments	9d28cc4d-0e82-4330-9564-96b40a58248c/RTB565
run RNA probes (HCR)	Molecular Instruments	9d28cc4d-0e82-4330-9564-96b40a58248c/RTB564
cad RNA probes (HCR)	Molecular Instruments	d5cdac09-6920-42eb-b229-b5d2421b995c/RTB831
tll RNA probes (HCR)	Molecular Instruments	d5cdac09-6920-42eb-b229-b5d2421b995c/RTB299
grh RNA probes (HCR)	Molecular Instruments	6bb0a64d-d4b8-4b1a-a83b-7d76fe5d9a77/PRR869
sna RNA probes (HCR)	Molecular Instruments	4614/E928

CadN RNA probes (HCR)	Molecular Instruments	6bb0a64d-d4b8-4b1a-a83b-7d76fe5d9a77/PRR868
htl RNA probes (HCR)	Molecular Instruments	6bb0a64d-d4b8-4b1a-a83b-7d76fe5d9a77/PRB870
sim RNA probes (HCR)	Molecular Instruments	9d28cc4d-0e82-4330-9564-96b40a58248c/RTB560
lacZ RNA probes (HCR)	Molecular Instruments	d5cdac09-6920-42eb-b229-b5d2421b995c/RTB830
bnk RNA probes (HCR)	Molecular Instruments	5fa8f306-142e-4909-8555-3a57ae81b8a5/RTF902
dhd RNA probes (HCR)	Molecular Instruments	5fa8f306-142e-4909-8555-3a57ae81b8a5/RTF901
DNaseII RNA probes (HCR)	Molecular Instruments	94ed6100-de8d-4db1-82ca-3d3a69c9fb59/RTF683
sog RNA probes (HCR)	Molecular Instruments	3285/C529
bap RNA probe	Trisnadi and Stathopoulos[S3]	N/A
aos RNA probe	Trisnadi and Stathopoulos[S3]	N/A
ATGATGATGAACGCCTTCAT	This study	opa-F
AAGTAATACGACTCACTATAGGGAGATGTATGCGTCCGCTTGTGGA	This study	opa-R
AATCACTGGCGGTCGAACAA	This study	run:FP1
TAATACGACTCACTATAGATACGGATGGAAGGCGTGTG	This study	run:RP1T7
ATTAACCCTCACTAAAGGGAGCAGATCCCTATCTTCACGC	This study	byn-F
TAATACGACTCACTATAGGTGGGATAGGAGAACACGGAC	This study	byn-R
AGGAGCGCGAGACAAGTCT	This study	odd-F

AAGTAATACGACTCACTATAGGGA GATGTATGCGTCCGCTTGTGGA	This study	odd-R
TAGCGCTCACAGTCTCCACTTTCA	This study	slp2-F
AAGTAATACGACTCACTATAGGGA GACCACCGAGAGTTGCCTTTGAT	This study	slp2-R
CGATTAAGACGCACCACAGTTC	This study	oc-F
TAATACGACTCACTATAGCATATTC GCGTACTTATCCTGC	This study	oc-R
CCTTTACAAACTGCCCAAGC	This study	DNaseII-F
TAATACGACTCACTATAGTTGTCG TAGTTGGTGACCAG	This study	DNaseII-R
GCAATGGTCGCTTGGAAATC	This study	gcm-F
TAATACGACTCACTATAGCTGTTG ACTGGGTGATATG	This study	gcm-R
GCTATCCCATGACGCGTTCG	This study	pxb-F
TAATACGACTCACTATAGCTTGGT TTCGGTTGGGTTAGC	This study	pxb-R
ATAAGGACATACGTGCCCAGATC	This study	comm-F
TAATACGACTCACTATAGCAACAA CAACGACCAATGA	This study	comm-R
ATGAAGAACTCCCACGCG	This study	btn-F
TAATACGACTCACTATAGCTTGCT GCTCCTCCAGTT	This study	btn-R
GACTGTTACGCAGATTGTTCG	This study	mirr-F
TAATACGACTCACTATAGTAGAGT TACGATGCACCGATG	This study	mirr-R
CTGTGCGTCGGAAGTGAATC	This study	phm-F
TAATACGACTCACTATAGACAACC TAATCCTGCACCAC	This study	phm-R

SUPPLEMENTAL REFERENCES LIST

[S1] Karaiskos, N., Wahle, P., Alles, J., Boltengagen, A., Ayoub, S., Kipar, C., Kocks, C., Rajewsky, N., and Zinzen, R.P. (2017). The embryo at single-cell transcriptome resolution. Science 358, 194–199.

[S2] Seroka, A., Lai, S.-L., and Doe, C.Q. (2022). Transcriptional profiling from whole embryos to single neuroblast lineages in Drosophila. Dev. Biol. 489, 21–33.

[S3] Trisnadi, A., Stathopoulos, A. (2014). Ectopic expression screen identifies genes affecting Drosophila mesoderm development including the HSPG Trol. G3. Dec 23;5(2):301-13.